Electronic Supplementary information

Designing Dual Emitting Cores for Highly Efficient Thermally Activated Delayed Fluorescent Emitters

Danqing Wei,[ab] Fan Ni,[a] Zhongbin Wu,[c] Zece Zhu,[a] Yang Zou,[b] Kailu Zheng,[a] Zhanxiang Chen,[a] Dongge Ma*[cd] and Chuluo Yang*[ab]

[a] Hubei Key Lab on Organic and Polymeric Optoelectronic Materials, Department of Chemistry, Wuhan University, Wuhan, 430072, China. *E-mail: clyang@whu.edu.cn

[b] Shenzhen Key Laboratory of Polymer Science and Technology, College of Materials Science and Engineering, Shenzhen University, Shenzhen, 518060, China.

[c] State Key Laboratory of Polymer Physics and Chemistry, Changchun Institute of Applied Chemistry, University of Chinese Academy of Sciences Changchun, Changchun 130022, China. *E-mail: mdg1014@ciac.ac.cn

[d] Institute of Polymer Optoelectronic Materials and Devices, State Key Laboratory of Luminescent Materials and Devices, South China University of Technology, Guangzhou, 510640, China.

Calculation

The ground state molecular structures were optimized at the B3LYP/6-31g(d) level of theory. Energy gaps between first singlet state (S_1) and triplet state (T_1) were calculated by using the TD-LC-ωPBE/6-31g(d) level of theory on the optimized geometry. The rate constants k_{p}, k_{d}, k_{ISC}, k_{RISC}, k_r and k_{nr} were estimated by using the following formulas with the assumption that $k_{RISC} \gg k_{r,T} + k_{nr,T}$.

$$k_{\mathrm{p}} = \frac{1}{\tau_{\mathrm{p}}} \quad (1)$$

$$k_{\mathrm{d}} = \frac{1}{\tau_{\mathrm{d}}} \quad (2)$$

$$k_{\mathrm{r,s}} = \Phi_{\mathrm{p}} k_{\mathrm{p}} + \Phi_{\mathrm{d}} k_{\mathrm{d}} \approx \Phi_{\mathrm{p}} k_{\mathrm{p}} \quad (3)$$

$$k_{\mathrm{RISC}} \approx \frac{k_{\mathrm{p}} k_{\mathrm{d}} \Phi}{k_{\mathrm{r,s}}} \quad (4)$$

$$k_{\mathrm{ISC}} \approx \frac{k_{\mathrm{p}} k_{\mathrm{d}} \Phi_{\mathrm{d}}}{k_{\mathrm{RISC}} \Phi_{\mathrm{p}}} \quad (5)$$

$$k_p = k_r + k_{nr} + k_{ISC} \quad (6)$$

Synthesis of the intermediates

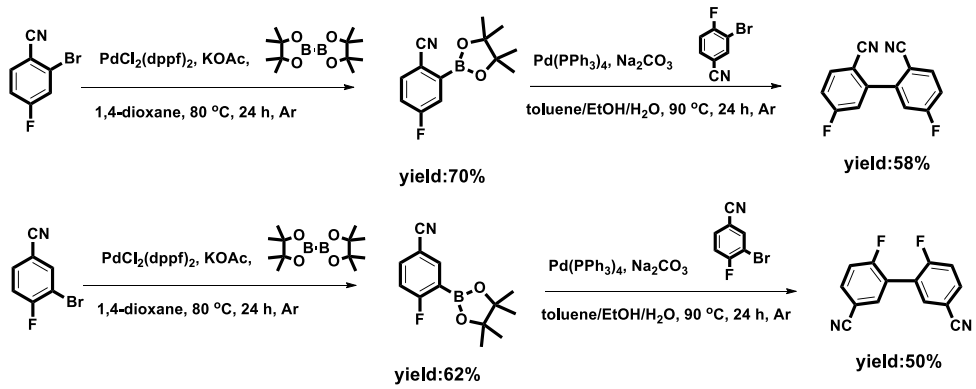

4-fluoro-2-(4,4,5,5-tetramethyl-1,3,2-dioxaborolan-2-yl)benzonitrile

2-bromo-4-fluorobenzonitrile (2.94 g, 15 mmol), $PdCl_2(dppf)_2$ (330 mg, 0.45 mmol), KOAc (4.41 g, 45 mmol) and 4,4,4',4',5,5,5',5'-octamethyl-2,2'-bi(1,3,2-dioxaborolane) (4.57 g, 18 mmol) were dissolved in dry 1,4-dioxane (80 mL) under argon atmosphere. The mixture was stirred at 80°C for 24 hours, then cooled down to room temperature.

The reaction mixture was slowly poured into water and extracted with 100 mL ethyl acetate for 3 times. The organic phase was dried over anhydrous Na_2SO_4, filtered and concentrated under reduced pressure. The crude product was purified by column chromatography with ethyl acetate/petroleum ether (v/v = 1/15) as eluent. Finally, the colorless oil was obtained with a yield of 70%. ^{1}H NMR (400 MHz, $CDCl_3$) δ (ppm): 1.38 (s, 12H), 7.19-7.24 (m. 1H), 7.55-7.58 (m, 1H), 7.70-7.73 (m, 1H).

5,5'-difluoro-[1,1'-biphenyl]-2,2'-dicarbonitrile

2-bromo-4-fluorobenzonitrile (2.22 g, 11 mmol), 4-fluoro-2-(4,4,5,5-tetramethyl-1,3,2-dioxaborolan-2-yl)benzonitrile (4.14 g, 10 mmol), $Pd(PPh_3)_4$ (60 mg, 0.05 mmol) and Na_2CO_3 (4.24 g, 40 mmol) were stirred in a mixture of toluene, ethanol and H_2O (v:v:v = 4:2:1) at 90°C for 24 hours under argon atmosphere. After cooling down to room temperature, the mixture was slowly added into water and extracted with 100 mL CH_2Cl_2 for 3 times. The organic phase was dried with anhydrous Na_2SO_4, filtered and concentrated under reduced pressure. The crude product was purified by column chromatography with petroleum ether/CH_2Cl_2 (v/v = 1/1) as eluent. Finally, the white powder was obtained with a yield of 58%. ^{1}H NMR (400 MHz, $CDCl_3$) δ (ppm): 7.27-7.35 (m, 4H), 7.85-7.89 (d, J = 8.0 Hz, 2H).

4-fluoro-3-(4,4,5,5-tetramethyl-1,3,2-dioxaborolan-2-yl)benzonitrile

3-bromo-4-fluorobenzonitrile (2.94 g, 15 mmol), $PdCl_2(dppf)_2$ (330 mg, 0.45 mmol), KOAc (4.41 g, 45 mmol) and 4,4,4',4',5,5,5',5'-octamethyl-2,2'-bi(1,3,2-dioxaborolane) (4.57 g, 18 mmol) were dissolved in dry 1,4-dioxane (80 mL) under argon atmosphere. The mixture was stirred at 80°C for 24 hours, and then cooled down to room temperature. The reaction mixture was slowly poured into water and extracted with 100 mL ethyl acetate for 3 times. The organic phase was dried over anhydrous Na_2SO_4, filtered and concentrated under reduced pressure. The crude product was purified by column chromatography with ethyl acetate/petroleum ether (v/v = 1/15) as

eluent. Finally, the colorless oil was obtained with a yield of 62%. ^{1}H NMR (400 MHz, $CDCl_3$) δ (ppm): 1.26 (s, 12H), 7.15 (t, J = 8.0 Hz, 1H), 7.72-7.76 (m, 1H), 8.08-8.10 (m, 1H).

6,6'-difluoro-[1,1'-biphenyl]-3,3'-dicarbonitrile

2-bromo-4-fluorobenzonitrile (2.22 g, 11 mmol), 4-fluoro-2-(4,4,5,5-tetramethyl-1,3,2-dioxaborolan-2-yl)benzonitrile (4.14 g, 10 mmol), $Pd(PPh_3)_4$ (60 mg, 0.05 mmol) and Na_2CO_3 (4.24 g, 40 mmol) were stirred in a mixture of toluene, ethanol and H_2O (v:v:v = 4:2:1) at 90°C for 24 hours under argon atmosphere. After cooling down to room temperature, the mixture was slowly added into water and extracted with 100 mL CH_2Cl_2 for 3 times. The organic phase was dried with anhydrous Na_2SO_4, filtered and concentrated under reduced pressure. The crude product was purified by column chromatography with petroleum ether/CH_2Cl_2 (v/v = 1/1) as eluent. Finally, the white powder was obtained with a yield of 50%. ^{1}H NMR (400 MHz, $CDCl_3$) δ (ppm): 7.33-7.37 (m, 2H), 7.73-7.80 (m, 4H).

Supplementary figure

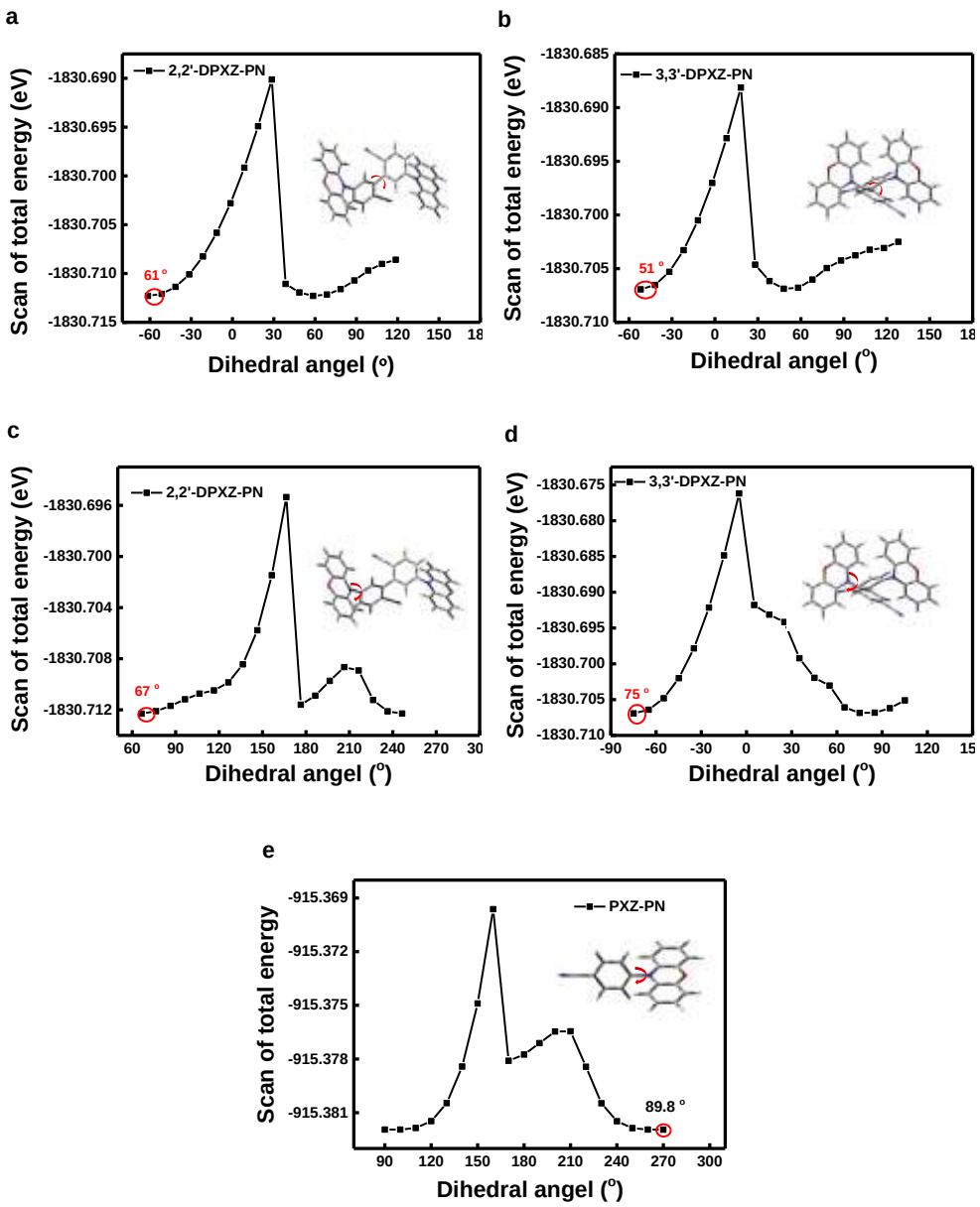

Fig. S1 The dihedral angels between the linked two phenyls (α) of **2,2′-DPXZ-PN** (a) and **3,3′-DPXZ-PN** (b); the dihedral angles between PXZ and the connected phenyl (β) of **2,2′-DPXZ-PN** (c), **3,3′-DPXZ-PN** (d) and **PXZ-PN** (e).

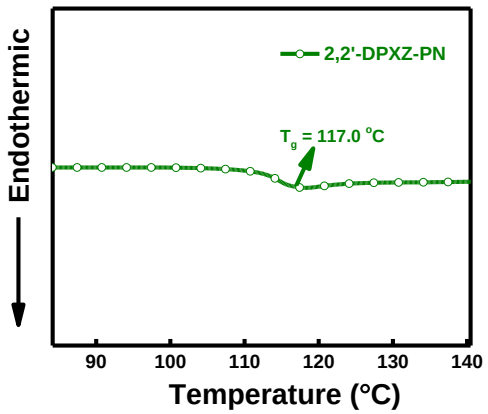

Fig. S2 DSC curves of **2,2'-DPXZ-PN**.

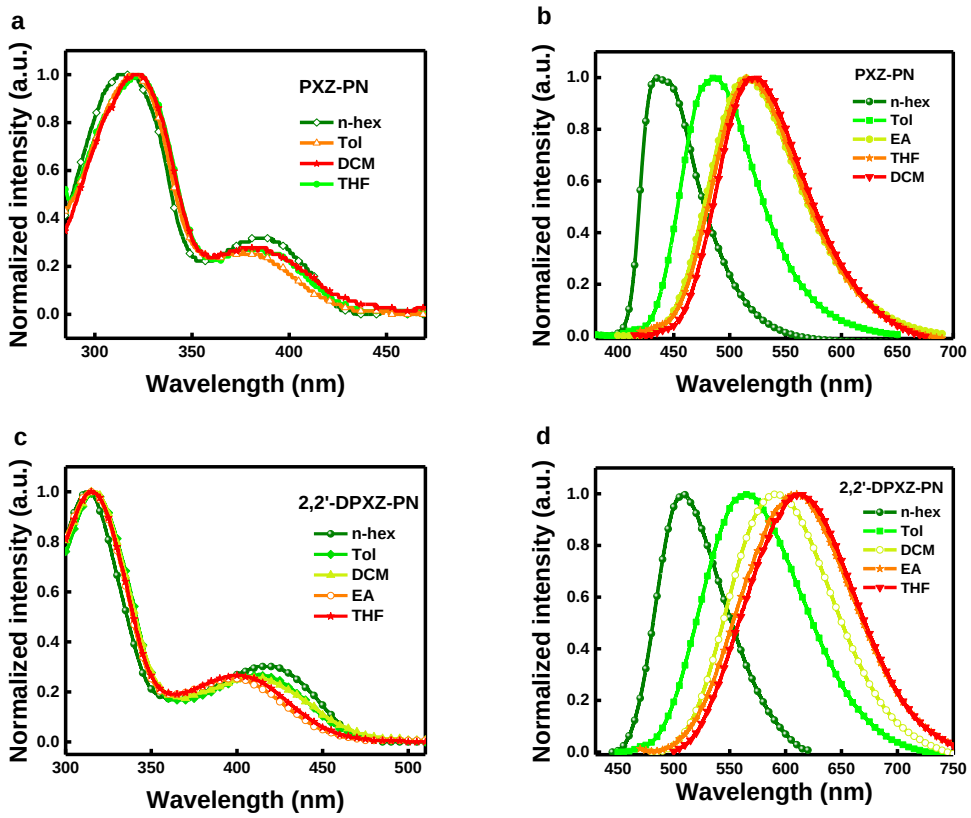

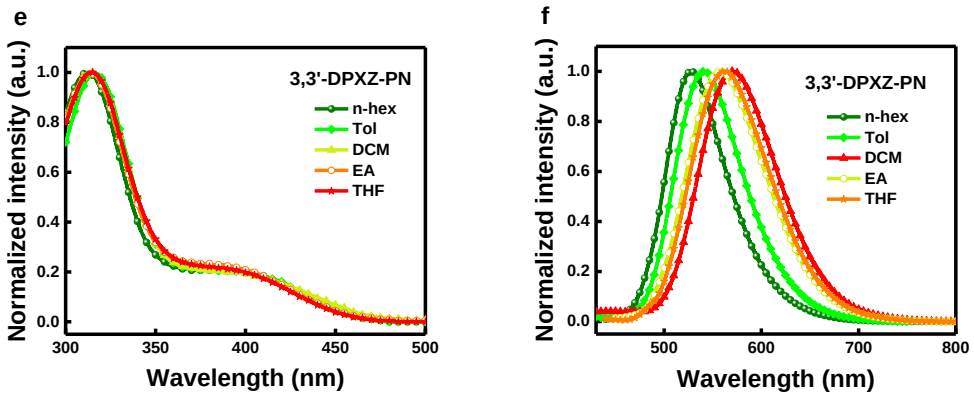

Fig. S3 UV-Vis absorption spectra (a), (c), (e) and steady-state fluorescence spectra (b), (d), (f) of **PXZ-PN**, **2,2′-DPXZ-PN** and **3,3′-DPXZ-PN** in different solvents. (n-hex = n-hexane, Tol = toluene, DCM = dichloromethane, EA = ethyl acetate and THF = tetrahydrofuran, c = 1.0 × 10^{-5} M).

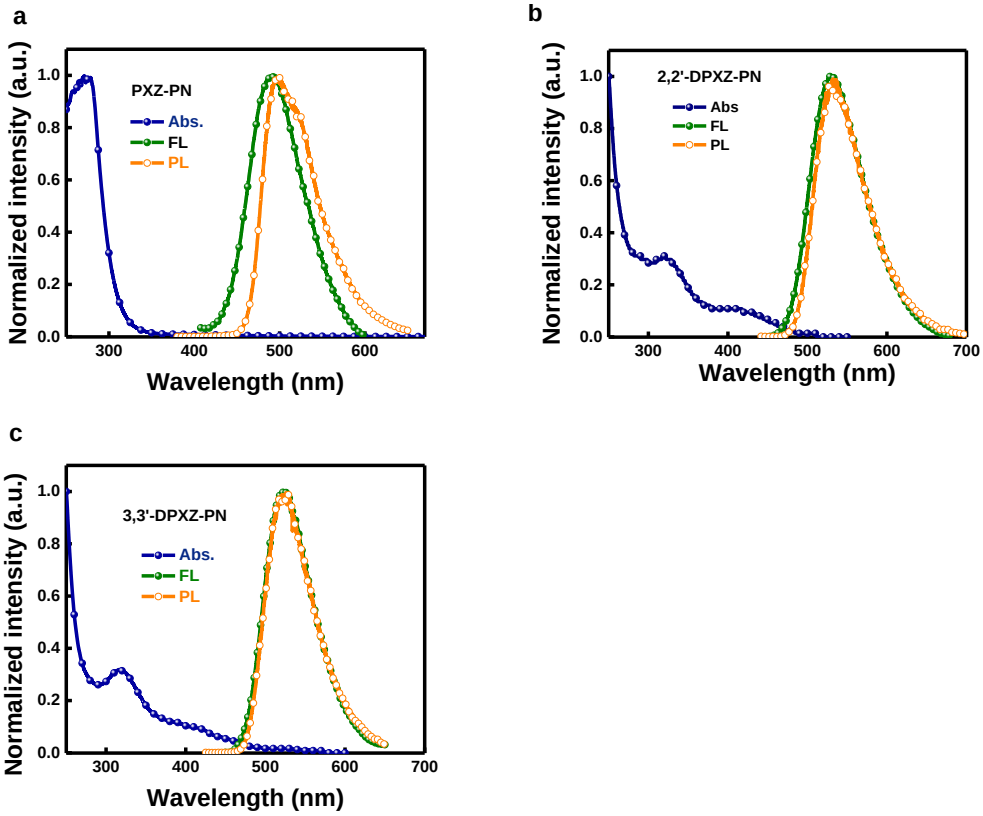

Fig. S4 The UV-Vis absorption spectra in neat film, fluorescence spectra at room temperature and phosphorescence spectra at 77 K in doped film of **PXZ-PN** (a), **2,2′-DPXZ-PN** (b) and **3,3′-DPXZ-PN** (c).

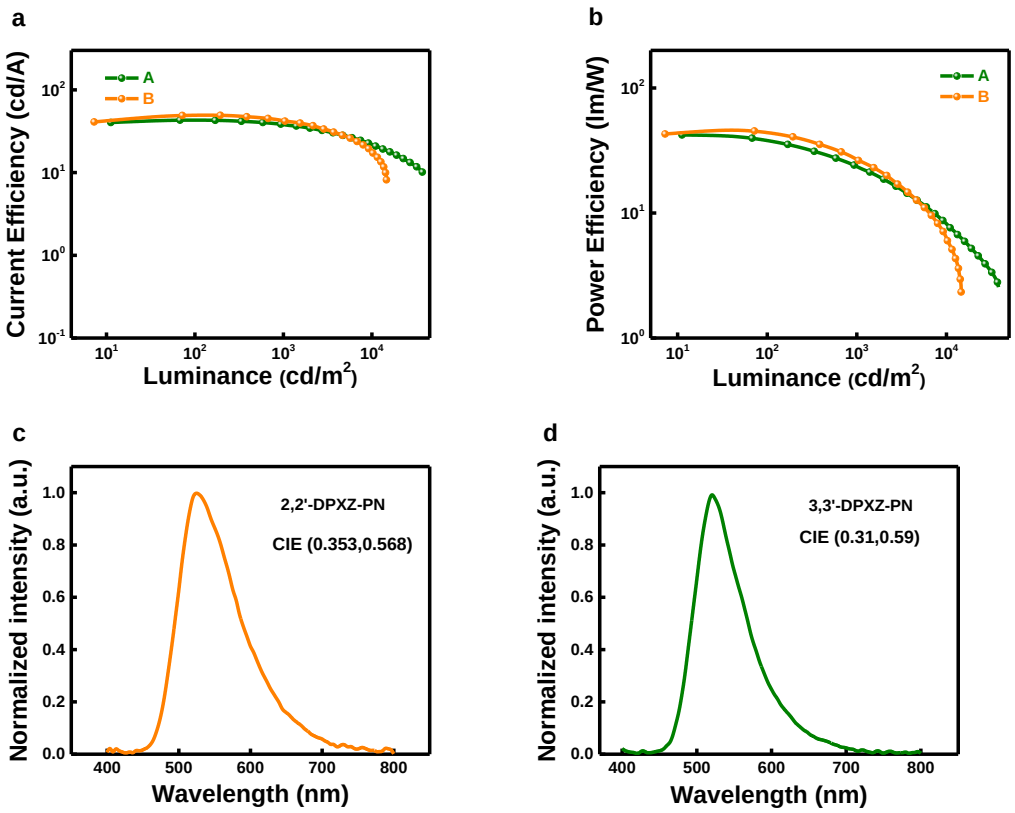

Fig. S5 The current efficiency (a) and power efficiency (b) versus luminance curves of device A and B, the electroluminescence spectra of **2,2′-DPXZ-PN** and **3,3′-DPXZ-PN**.

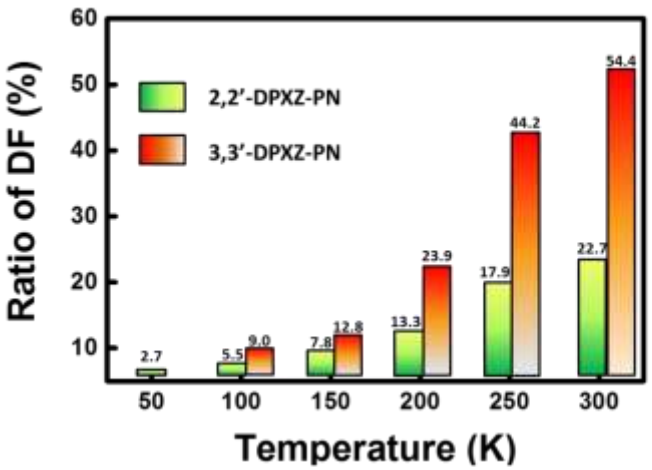

Fig. S6 The percentages of delayed fluorescence of **2,2′-DPXZ-PN** and **3,3′-DPXZ-PN** in 10 wt% doped CBP films in argon atmosphere from 77 to 300 K.

Table S1 The emission peak of **2,2′-DPXZ-PN** and **3,3′-DPXZ-PN** in different solvents.

Compounds	**λ/nm (n-hex)**	**λ/nm (tol)**	**λ/nm (THF)**	**λ/nm (DCM)**
2,2'-DPXZ-PN	**509**	**564**	**590**	**612**
3,3'-DPXZ-PN	**517**	**540**	**557**	**562**

Table S2 The dipole moment of **2,2′-DPXZ-PN** and **3,3′-DPXZ-PN** in ground state and excited states of different solvents.

compounds	μ_g**/D**	μ_e**/D n-hex**	$\Delta\mu$***/D***	μ_e**/D tol**	$\Delta\mu$**/D**	μ_e**/D dcm**	$\Delta\mu$**/D**	μ_e**/D THF**	$\Delta\mu$**/D**
2,2′-DPXZ-PN	2.31	21.42	19.11	21.77	19.46	23.68	21.37	23.44	21.13
3,3′-DPXZ-PN	2.14	12.98	10.84	13.31	11.17	15.01	12.87	14.84	12.70

Table S3 The lifetimes of **2,2′-DPXZ-PN** and **3,3′-DPXZ-PN** in 10 wt% doped CBP films in argon atmosphere from 77 to 300 K.

Compounds	77K	100K	150K	200K	250K	300K
2,2′-DPXZ-PN	1.0 μs	2.5 μs	3.4 μs	4.5 μs	5.5 μs	5.0 μs
3,3′-DPXZ-PN	-	3.6 μs	6.9 μs	9.9 μs	10.8 μs	8.9 μs